Euro. Jnl of Applied Mathematics (1998), *vol.* 9, *pp.* 327–350. Printed in the United Kingdom

Evolution of self-similarity, and other properties of waiting-time solutions of the porous medium equation: the case of viscous gravity currents

JULIO GRATTON and CLAUDIO VIGO

INFIP(LA)-Laboratorio de Física del Plasma, Facultad de Ciencias Exactas y Naturales, Universidad de Buenos Aires, Pabellón I. Ciudad Universitaria (1428) Buenos Aires, Argentina
(email: jgratton@tinfip.lfp.uba.ar)

(Received 30 July 1996 and in revised form 4 June 1997)

The one-dimensional porous medium equation $h_t = (h^m h_x)_x$ $(m > 0)$ admits waiting-time solutions, whose front remains motionless during a finite time interval t_w before starting to move. We consider a family of initial value problems, and investigate the asymptotics, close to the front and near start-up, which we expect to be self-similar. We obtain numerical solutions for viscous gravity currents ($m = 3$) and power-law initial conditions ($h \propto x^p$, h is proportional to the thickness of the fluid, x is the distance to the front). We find that: (a) if $p < 2/3$ the front starts moving immediately, (b) if $p = 2/3$ the front remains motionless during a finite time, (c) if $p > 2/3$ one obtains waiting-time solutions in which a moving corner layer (a small interval Δx in which h_x varies strongly) appears behind the front; the front starts moving when it is overrun by the corner layer. The corner layer strengthens (Δx reduces and the variation of h_x increases) as it approaches the front. Our initial conditions produce waiting-time solutions whose front starts moving with nonzero velocity. We determine $t_w(p)$ and study the motion of the corner layer and the front, as well as other properties of the solutions. We compare the results with the theoretical upper and lower bounds of t_w. We investigate the asymptotics of the numerical solutions for $p > 2/3$, close to the corner layer and the front, and near start-up. To represent this asymptotics various kinds of similarity solutions are available, that can be classified according to the self-similarity exponent δ. We find that only two types (called L and A) are relevant. The L solutions correspond to $1 < \delta < 13/10$, and have an infinite series of corner layers that accumulate at the front. The part of these solutions behind the first corner layer of the series represents the asymptotics of the numerical solutions in a domain that excludes the region between the corner layer and the front, for a time interval excluding the neighbourhood of start-up. The A solutions have $\delta \leqslant 1$, and represent the evolution of the strong corner layer that is arriving at the front. The numerical evidence shows that the constant front velocity solution (type A with $\delta = 1$) describes the asymptotics close to, and including start-up, so that the motion of the corner layer joins smoothly with that of the front.

1 Introduction

We consider the one-dimensional porous medium equation with plane symmetry:

$$h_t = (h^m h_x)_x, \tag{1}$$

($h \equiv h(x, t) \geqslant 0, m > 0$). This equation governs a variety of phenomena: unconfined groundwater flow ($m = 1$, Polubarinova-Kochina, 1962; Eagleson, 1970; Peletier, 1981),

https://doi.org/10.1017/S095679259700329X Published online by Cambridge University Press

percolation of gases in porous media ($m = \gamma \geqslant 1$, γ is the ratio of specific heats (see Muskat, 1937; Gilding & Peletier, 1976; Vázquez, 1983, etc.), thermal conduction in plasmas ($m = 5/2$; Zel'dovich & Raizer, 1966), viscous gravity currents over a plane rigid surface ($m = 3$, $h = (g/3\nu)^{1/3} H$, H is the thickness of the fluid, ν the kinematic viscosity, g the acceleration of gravity (see Buckmaster, 1977; Huppert, 1982; Gratton & Minotti, 1990), thermal conduction in multiply ($m = 4.5$–5.5) and totally ionized gases ($m = 13/2$) (see Marshak, 1958; Zel'dovich & Raizer, 1966; Pert, 1977; Larsen & Pomraning, 1980, etc.). We take the viscous gravity currents as a 'model' case, since they have been studied experimentally (Thomas *et al.*, 1981; Gratton *et al.*, 1992; Marino *et al.*, 1995).

With the substitution $\eta = h^m$, $\tau = t/m$ (1) takes the form

$$\eta_\tau = \eta_x^2 + m\eta\eta_{xx}, \tag{2}$$

showing that the evolution of η is the result of the combined effect of nonlinear wave propagation and nonlinear diffusion. The nonlinear diffusion term of (2) leads to the occurrence of fronts (also called interfaces in the mathematical literature; the suffix f will denote quantities relating to a front). The motion of a front is continuous in time and its direction never reverses. For example, if $\eta(x, \tau_0) = 0$ for $x \geqslant x_f(\tau_0)$, then for any $\tau > \tau_0$ one has $\eta(x, \tau > \tau_0) = 0$ for $x \geqslant x_f(\tau) \geqslant x_f(\tau_0)$. Another typical feature is the occurrence of corner layers (i.e. small intervals Δx in which η_x varies rapidly), as a result of the combined effect of the nonlinear term that tends to produce discontinuities of η_x (corner shocks), and the diffusion term that smoothens strong variations of η_x. We shall designate by a suffix c the quantities pertaining to a corner layer.

An important property of the porous medium equation is the occurrence of waiting-time solutions. Let us assume that the process begins at $t = t_i$; and the initial condition is $h(x, t_i) = g(x)$ ($g(x) \geqslant 0$). For appropriate $g(x)$, the front may remain motionless during a finite interval t_w ($x_f(t) = x_f(t_i)$ for $t \leqslant t_i + t_w$), while changes occur behind it (waiting stage). In the following we assume that: (a) $t_i = -t_w$, so that the front begins to move at $t = 0$ (start-up), the subsequent interval will be called moving stage; (b) $g(x) \not\equiv 0$ in the interval $0 < x \leqslant x_0$, and $g(x) = 0$ in $x \leqslant 0$ so that $x_f(-t_w) = 0$; (c) the solution is defined for $-\infty < x \leqslant x_0$. Then the velocity of the front $\dot{x}_f(t)$ cannot be positive ($\dot{x}_f(t) \leqslant 0$). At $x = x_0$ and $t > -t_w$ we assume the boundary condition $h_x(x_0, t) = 0$. The initial condition determines a scale h_0 of $h(x, -t_w)$ (h_0 is any typical value of $g(x)$, for example its maximum value), a spatial scale x_0, and a time scale $t_0 \equiv x_0^2 h_0^{-m}$. These are the only scales of the phenomenon (in particular, t_0 is the scale of the waiting-time). Many theoretical papers have dealt with waiting-time solutions (see, for example, Aronson, 1970; Knerr, 1977; Kamin, 1980; Lacey *et al.*, 1982; Kath & Cohen, 1982; Lacey, 1983; Aronson *et al.*, 1985; etc.), but few experimental results (Thomas *et al.*, 1991; Gratton *et al.*, 1992; Marino *et al.*, 1995) and numerical analyses (see, for example, Gratton & Vigo, 1994a) are available. We are interested here in the connection between the initial condition and the waiting-time behavior; to this purpose we consider initial conditions of the form (K, p are positive constants):

$$g(x) = Kx^p \quad \text{if} \quad 0 \leqslant x \leqslant x_0, \quad g(x) = 0 \quad \text{if} \quad x < 0. \tag{3}$$

There are no general theoretical formulae for t_w, but theorems that establish upper and lower bounds have been derived (see Aronson *et al.* 1981; Kath & Cohen, 1982; Lacey *et al.* 1982; Vázquez, 1984). In the case $m \ll 1$, with initial conditions of the form $g(x) \propto x^p$,

https://doi.org/10.1017/S095679259700329X Published online by Cambridge University Press

Kath & Cohen (1982) have shown that there is a non-vanishing waiting time if $p \geqslant 2/m$ (this result holds for any $m > 0$; see Vázquez, 1984), and that a corner layer (if $p > 2/m$) or a corner shock (if $p = 2/m$) appears in the solution.

We are particularly concerned with the asymptotics near the front and close to start-up ($|x| \ll x_0, |t| \ll t_w, t_0, |h| \ll h_0$). In this domain, h_0, x_0 and t_0 cannot be used as scales, so that we conjecture that the solution will be self-similar, depending on the variable $\zeta = x/bt^\delta$ (b and δ are constants). Lacey *et al.* (1982) have given prescriptions to construct a set of self-similar waiting-time solutions (that we shall henceforth name LOT solutions), whose self-similarity exponent δ may take any value $\delta > 1$. Gratton & Vigo (1994b) made a detailed study of the properties of the LOT solutions; they are of three types (L, S and N in the following): (a) if $1 < \delta < 1 + m/2(m+2)$, h and u display an infinite succession of corner layers, with an accumulation point at the front (type L); (b) if $\delta > 1 + m/2(m+2)$, the solutions have no corner layer (types S and N). In addition to the LOT solutions we shall show that there is another family of self-similar solutions (which we call A solutions), corresponding to $\delta \leqslant 1$, that describe a strong corner layer (we call 'strong' a corner layer whose thickness Δx is very small) as it approaches and overtakes the waiting front. The constant velocity front solution is an important special case ($\delta = 1$) of this family. Theory does not determine δ and b; they depend on the initial conditions in a way not known beforehand, and can be found only by an experiment, or by solving (numerically) the initial value problem, and following the evolution of the phenomenon until some asymptotic regime is achieved near the front and close to the start-up time. We want to stress that there is no theoretical argument that guarantees that the initial value problem (1), (3) will really develop a self-similar asymptotics in this domain: it might as well happen that no self-similar behavior occurs (of course, the long-time behavior after start-up of our solutions approaches the self-similar 'point source' solution). Only experimental or numerical evidence can give an answer. To clarify these issues is one of the objectives of the present investigation. We shall show below that the numerical solutions have a self-similar asymptotics (as already suggested by experiments on the viscous spreading of linear ramps, see Marino *et al.*, 1995), but their development involves subtle and surprising features. In this connection, we must mention the important theorems derived by Lacey (1983) and Aronson *et al.* (1985) about the initial motion of the front of a waiting-time solution. The relevant result is that $\dot{x}_f$ is discontinuous at start-up for a class of initial profiles, that includes those of the form $g(x) \propto x^p$, with $p > 2/m$. More precisely, and considering the solutions of (1), (3) with $p > 2/m$, it can be proved (Aronson *et al.*, 1985) that the quantity $c \equiv \dot{x}_f(t = 0+)$ satifies the inequality

$$\frac{|c|\, t_0}{x_0} \geqslant \frac{c^* t_0}{x_0} \equiv \frac{1}{9(m+1)^2}. \tag{4}$$

A consequence of this property is that the LOT solutions, for which $\dot{x}_f$ is continuous at start-up, cannot describe the asymptotics of this initial value problem in domains that include $t = 0$. On the other hand, the A solutions can satisfy (4) and are candidates to describe the asymptotics in the neighbourhood of $t = 0$ ($|c|$ can take any value if $\delta = 1$, and $|c| = \infty$ if $\delta < 1$). Therefore, if the asymptotics we are seeking is self-similar at all, it must correspond to a type A solution. Indeed, the numerical solutions tend to a constant velocity ($\delta = 1$) type A self-similarity. In addition, we shall show that there exists a space-time

https://doi.org/10.1017/S095679259700329X Published online by Cambridge University Press

domain near (but not too near) to the front and close to (but excluding) $t = 0$ in which a type L solution is in excellent agreement with the numerical solution.

In this paper we solve numerically the initial value problem (1), (3) for $m = 3$, since this case (viscous gravity currents) has been investigated in the laboratory. We find that the solutions harmonize with the predictions of theory, but in addition yield a bounty of new information. The present results suggest topics for further theoretical research and may be useful for applications. When $p > 2/3$ we obtain the waiting-time behaviour, determine t_w, and study the formation and evolution of the corner layer as well as other properties of the solutions. In addition, the analysis of the asymptotics reveals two domains in which the numerical solution has a different behavior. The first one, in which the solution displays a $\delta = 1$ type A asymptotics, occurs very close to the front and near $t = 0$ ($|x| < \epsilon x_0, |t| < \epsilon t_w, \epsilon \ll 1$). The second domain extends in the intervals $\epsilon x_0 \ll |x| \ll x_0$, $\epsilon t_w \ll |t| \ll t_w$, where $|h| \ll h_0$; there the behavior is of type L, with $\delta = \delta(p) > 1$. In this domain we determine the relationship between δ and p. The present results are in good agreement with the experiments on viscous gravity currents (Thomas *et al.*, 1991; Gratton *et al.*, 1992; Marino *et al.*, 1995) produced by the spreading of linear ramps and with other numerical solutions for $p = 1$ (Del Carmen & Ferreri, 1995; Marino *et al.*, 1995), but the very high accuracy and spatial resolution of our calculations and the absence of the perturbing effects always present in the experiments, reveals many fine details not observed previously and allows more stringent checks of the self-similarity in the asymptotic regime.

2 Theory

In this section we shall summarize some relevant theoretical results on waiting-time solutions, emphasizing those related to initial conditions of the type $h \propto x^p$ and to the case of viscous gravity currents, but keeping m arbitrary for generality.

2.1 Influence of the initial conditions

When $m \to 0$, the diffusion term of (2) is small, and can be treated as a perturbation. To the lowest order (2) reduces to a first order nonlinear equation, that can be solved by the method of characteristics. With this approach Kath & Cohen (1982) investigated the solutions for $m \ll 1$, with initial conditions of the type (3). The result depends on the formation of a corner layer or a corner shock. If $0 < p < 2/m$, the front starts to move immediately. If $p = 2/m$, the front starts to move after a time interval $t_w > 0$, and at start-up a corner shock appears at the front. If $p > 2/m$ there is a waiting time $t_w > 0$ during which a corner layer appears behind the front; this corner layer moves towards the front becoming progressively stronger; start-up occurs when the front is overtaken by the corner layer, whose thickness vanishes at this moment. Vázquez (1984) considered arbitrary m and proved a necessary and sufficient condition for $t_w > 0$, that in the case of our initial conditions (3) is precisely $p > 2/m$. According to these results, start-up occurs immediately ($t_w = 0$) if $p < 2/m$.

2.2 Self-similar waiting-time solutions

In the present context we interpret, as is usual in physics, that the quantities that appear in the porous media equation (1) have dimensions, so that $[x] = L$, $[t] = T$ and $[h] = (L^2/T)^{1/m}$, but no constant dimensional parameter appears in (1). Then, when the initial and boundary

https://doi.org/10.1017/S095679259700329X Published online by Cambridge University Press

conditions of the problem involve no more than a single constant parameter b with independent dimensions, $[b] = LT^{-\delta}$, the solution of (1) is self-similar, i.e. it depends on the single independent variable $\zeta = x/bt^{\delta}$ (various examples of self-similar solutions of (1) are given by Barenblatt (1952), Barenblatt & Zel'dovich (1957), Pattle (1959), Pert (1977), Gilding & Peletier (1977a, b), Grundy (1979), Huppert (1982), Gratton & Minotti (1990), etc.). In the present problem the initial conditions introduce the parameters x_0, h_0 (and by dimensional reasons $t_w = \text{const} \times t_0$), then the solution of (1), (3) will not be self-similar. However, if one considers a waiting-time solution in a domain close to the front and near $t = 0$ ($|x| \ll x_0$, $|t| \ll t_w$, $|h| \ll h_0$) none of these parameters can be a scale for the phenomenon, so that we expect that the solution may approach a self-similar asymptotics. In this case δ is not known in advance, but can be found by requiring the existence of the solution (self-similarity of the second kind – see Barenblatt, 1979). This leads to a nonlinear eigenvalue problem (δ is then called an 'anomalous' exponent – see Aronson & Vázquez, 1994). The knowledge of δ fixes the dimensions of b, but is still not sufficient to determine its numerical value: it must be obtained studying experimentally or numerically the evolution of the initial value problem. In the case we are dealing with, it turns out that the eigenvalue spectrum is continuous. Then δ may in fact depend on the initial conditions of the non-self-similar problem (whose asymptotics is the self-similar solution of the second kind we are considering). In consequence (see Barenblatt & Zel'dovich, 1972) both δ and b must be obtained from the asymptotics of the initial value problem (1), (3).

We now recall briefly the construction of the self-similar waiting-time solutions of (1). To this end, we introduce the phase-plane (Z, V), writing (1) in the equivalent form $h_t = -(uh)_x$, $u = -h^{m-1}h_x$, with $h = [x^2 Z(\zeta)/t]^{1/m}$, $u = xV(\zeta)/t$ (in the case of a viscous gravity current u is the average horizontal velocity). The solutions are represented by integral curves $V(Z)$, which are solutions of the autonomous differential equation

$$\frac{dV}{dZ} = \frac{1}{m}\left(\frac{(\delta - V)}{Z} - Q(\beta V - 1)\right), \tag{5}$$

with $Q = -(2Z + mV)^{-1}$, $\beta = 2 + m$. The integral curves with $Z < 0$ represent solutions for $t < 0$ and those with $Z > 0$ correspond to solutions for $t > 0$. The space-time dependence of V, Z is obtained by integration of $d\lambda/dZ = Q$ with $\lambda = \ln|\zeta|$.

The features of the phase plane relevant for the self-similar waiting-time solutions are the singular points $O(0, 0)$, $A(0, \delta)$, $E(\infty, \infty)$, $B(-m/2\beta, 1/\beta)$, and a limit cycle L that may exist around B. We next outline their properties. Various drawings of the phase plane, for different δ, are displayed in the paper of Gratton & Minotti (1990).

2.2.1 *Singular points O, A, E*

The point O represents $\zeta = \infty$. For $Z < 0$ is a saddle where the single curve C_O ($V = V_O(Z)$) arrives. Near O, $V_O(Z \to 0) = (\delta^{-1} - 2)Z/m$, $h \propto x^{(2\delta-1)/m\delta}$, $u \propto -x^{(\delta-1)/\delta}$ (h, u do not depend on t for $x \to \infty$). In the half-plane $Z > 0$, O is a node and all the integral curves arriving there are tangent to C_O for $Z \to 0$. The point A is a saddle, through which two integral curves pass: $Z = 0$ and C_A. The latter is given near A by $V \approx \delta + (\beta\delta - 1)Z/4m\delta$; This solution has a moving front at $x_f = \zeta_f bt^{\delta}$ ($\zeta_f = \text{const.}$), near which $Z = m\delta(1 - \phi)$, $h \propto [t^{2\delta-1}(1-\phi)]^{1/m}$, $u \propto \phi/t$ ($\phi = \zeta/\zeta_f$). The node E represents $x = 0$; close to E the following formulae apply: $V \propto \sqrt{Z}$, $h \propto t^{(2\delta-1)/m}$, $u \propto t^{2\delta-1}$.

https://doi.org/10.1017/S095679259700329X Published online by Cambridge University Press

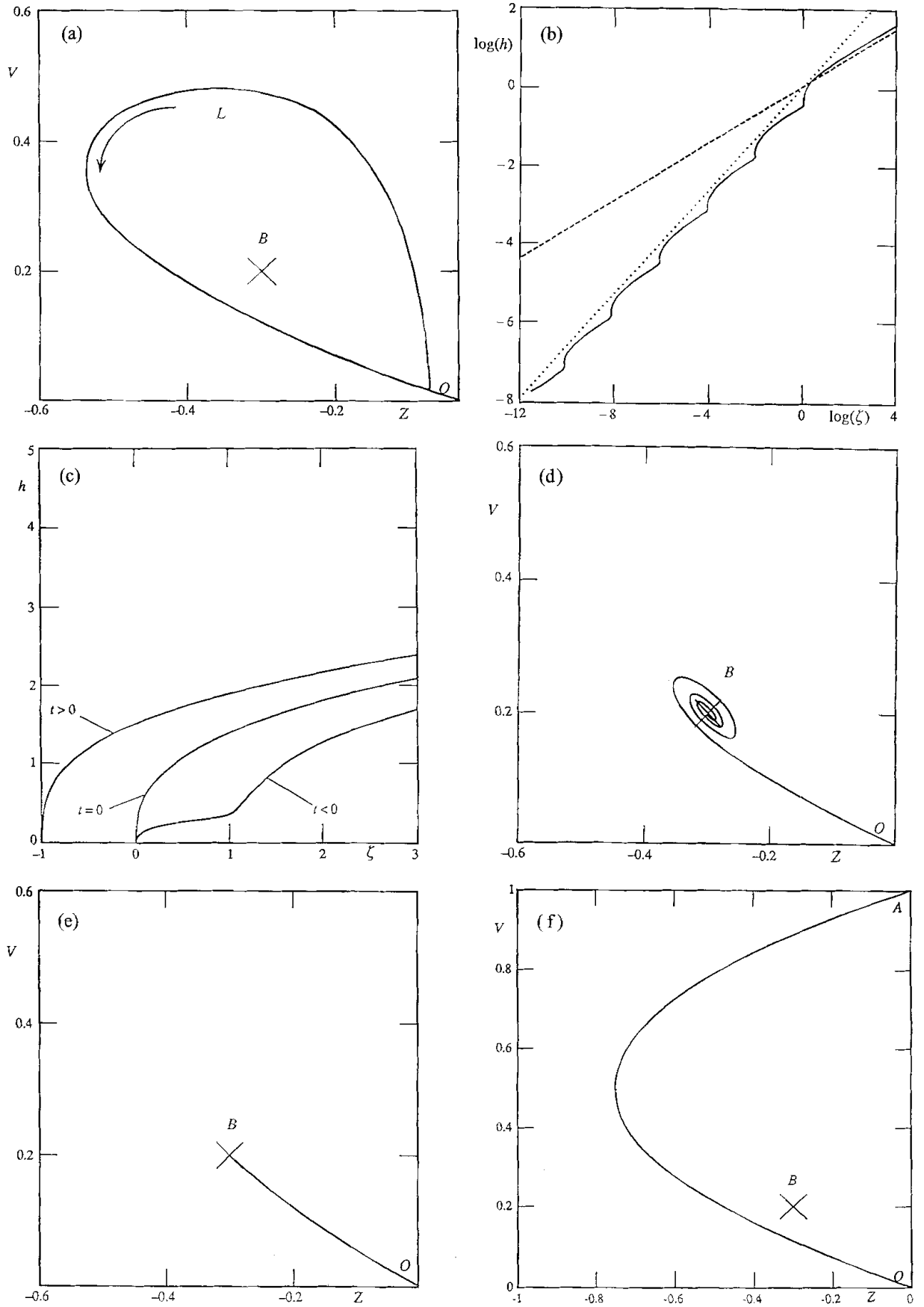

FIGURE 1. Some self-similar solutions discussed in the text: (a), (b), (c) integral curve, $\log h$ vs. $\log \zeta$ ($t < 0$, the straight dotted and broken lines show the asymptotic behaviour near B and O, respectively) and $h(\zeta)$ for a Type L solution ($\delta = 1.1$); (d) integral curve for a type S solution ($\delta = 1.4$); (e) integral curve for a type N solution ($\delta = 2.5$); (f) integral curve for the constant velocity solution ($\delta = 1$).

https://doi.org/10.1017/S095679259700329X Published online by Cambridge University Press

2.2.2 *The singular point B and the limit cycle*

Close to B the form of the solution is $h \propto (-x^2/t)^{1/m}$, $u \propto x/t$ $(t < 0)$. If $\delta < \delta_0$ $(\delta_0 = 1 + m/2\beta)$, B represents $\zeta = \infty$. If $\delta > \delta_0$, B represents a fixed (waiting) front at $\zeta = 0$; B is a node for $\delta \leqslant \delta_-$ or $\delta \geqslant \delta_+$ $(\delta_\pm = \delta_0 \pm \sqrt{(2m/\beta)})$; for $\delta_- \leqslant \delta < \delta_0$ it is a stable spiral point (the integral curves spiral counterclockwise towards B); for $\delta = \delta_0$, B is a centre in the linear approximation; for $\delta_0 \leqslant \delta < \delta_+$ it is an unstable spiral point (the integral curves spiral clockwise towards B).

If $\delta = 1$, the integral curves C_O and C_A coincide with the single curve C_{AO}, the parabola $Z = mV(V-1)$. If $\delta < 1$, C_A spirals towards B, leaving C_O to the left. When $\delta > 1$, C_O spirals towards B. If $1 < \delta < \delta_0$, both B and O represent $\zeta = \infty$, and there is a limit cycle L that surrounds B (a limit cycle exists only when $1 < \delta < \delta_0$, and the numerical evidence indicates that it is unique). In this case C_O as well as the integral curves going to B emanate from L, which represents a waiting-time front at $\zeta = 0$. When $\delta \to \delta_0$, L collapses into B and if $\delta \to 1$, L tends to C_{AO} and the segment OA of $Z = 0$.

2.2.3 *LOT solutions*

We now review the properties of the solutions of Lacey *et al.* (1982). For $t < 0$ the waiting front is at $x = 0$ and the solution must hold for arbitrarily large x, which implies that the integral curve must reach O. Appropriate curves C_O exist for any $\delta > 1$, and are of three types. If $1 < \delta < \delta_0$, C_O emanates from the limit cycle (L solutions). If $\delta_0 < \delta$ they begin at B: In this case C_O is a spiral (S solutions) if $\delta_0 < \delta < \delta_+$, or issues from the node (N solutions) if $\delta \geqslant \delta_+$. To extend the LOT solutions to $t > 0$, we use the same δ as for $t < 0$. Since now the solution has a moving front at $x = x_f(t) < 0$, it must be represented by the (unique) integral curve starting at A. As before, the solution must hold for arbitrarily large x, so that the integral curve must arrive to O. The corresponding integral trajectory lies in the half plane $Z > 0$ and consists of the curve AE, which represents the solution in the interval $x_f \leqslant x \leqslant 0$ and a curve EO which represents the solution for $0 \leqslant x < \infty$ (the continuity of h and u at $x = 0$ determines EO). The scale of ζ is arbitrary, and by convention we shall assume $\zeta_f = -1$.

A remarkable feature of the L solutions (Figure 1a–c) is that for δ close to 1, Z and V oscillate almost periodically with λ as $\lambda \to -\infty$, when C_O circles around L. Notice, however, that $h(\zeta)$ and $u(\zeta)$ are monotonic. We call $l (l < 0)$ the length of the period. In any period j $(j = 0, 1, \ldots)$, as the integral curve turns around L, there is an interval $\Delta\lambda \ll |l|$ close to $\lambda_j = jl$ (corresponding to the part of L nearer to A) where $dZ/d\lambda$ and $dV/d\lambda$ are large. This behaviour produces a kink in the profiles of $h(\zeta)$ and $u(\zeta)$, with all the properties of a corner layer. As $\delta \to 1$, one finds that $|l|$ increases and $\Delta\lambda \to 0$ so that $dZ/d\lambda$ and $dV/d\lambda$ tend to become discontinuous (corner shock). In consequence, the L solutions display an infinite succession of corner layers with an accumulation point at $\zeta = 0$. The first corner layer of this series occurs in the neighborhood of $\zeta_0 \approx |\zeta_f| = 1$, and the positions ζ_j of the successive ones follow a geometric progression of ratio e^l. The profiles of $h(\zeta)$ and $u(\zeta)$ due to successive turns around L differ by a scale factor e^l, but are otherwise almost identical (thus the solution has a structure – the corner layer – that repeats itself self-similarly: a self-similarity within a self-similarity!). It can also be seen in Figure 1 that in the intervals of

https://doi.org/10.1017/S095679259700329X Published online by Cambridge University Press

each turn, where $dZ/d\lambda$ and $dV/d\lambda$ are smaller, $h(\lambda)$ and $u(\lambda)$ repeat approximately the $\lambda \gg 1$ behavior (given by the part of C_O close to O). Notice also that the part of the solution nearer the front ($0 < \zeta < \zeta_0$) satisfies the inequalities $\alpha_1 < h(\zeta)\,\zeta^{-2/m} < \alpha_2$ where α_1, α_2 are two numbers and $0 < \alpha_1 < \alpha_2 < \infty$. As δ changes from 1 to δ_0, the amplitude of the oscillations reduces, the corner layers become weaker, and the period shortens (for example, in the case $m = 3$ ($\delta_0 = 13/10$), we find $l \approx -4.5$ for $\delta = 1.1$ and $l = -2.5$ for $\delta = 1.25$).

The solutions of types S and N do not have corner layer. In the S solutions ($\delta_0 < \delta < \delta_+$, see Figure 1 d) there are oscillations of the phase variables, but they quickly damp as the integral curve spirals to B, and $dZ/d\lambda$ and $dV/d\lambda$ never change rapidly. The corresponding undulations of h, u are very small and disappear near the front, where the solution is governed by B. Far from the front the solution is governed by O. The phase variables of the N solutions ($\delta > \delta_+$ see Figure 1 e) have a monotonic behaviour, governed by B for $\zeta \to 0$, and by O far from the front. The transition occurs around $\zeta \approx 1$.

2.2.4 *Type A solutions*

With the initial conditions (3), and $p > 2/3$, a corner layer develops during the waiting time. When $|t| \ll t_w$, the corner layer is strong and close to the front, and $h(x > x_c, t) \gg h(x < x_c, t)$. In consequence, its motion and the evolution of the solution in the domain $x_c < x < x_0$, tend to become independent of the profile in $0 < x < x_c$. This is seen in the numerical solutions, see below. In this regime there is an interval $x_c < x \ll x_0$ in which

$$h_0 \gg h(x > x_c, t) \gg h(x < x_c, t) \approx 0,$$

and the corner layer is equivalent to a moving front, since the influence of the vanishingly small h ahead is negligible. In this domain, no constant parameter arising from the initial and boundary conditions can be a scale of the solution. Then we expect a self-similar asymptotics (that need not be of the LOT type). If $0 < \delta \leqslant 1$, self-similar solutions with adequate properties exist (A solutions). These self-similarities are represented for $t < 0$ by the curve C_A that goes from A (that represents $x_c(t)$) to B (which represents a point of the domain far behind the corner layer). If $\delta = 1$, the type A solution is given by C_{AO} (see Figure 1f), and is a travelling wave that moves with constant velocity without changing shape:

$$h(x, t) = w(x, t) \equiv [cm(ct - x)]^{1/m}, \tag{6}$$

where $c = \text{const} \neq 0$ is the velocity of the front; this solution holds also for $t > 0$. If $\delta < 1$, the velocity of the front (and that of the corner layer) diverges at $t = 0$, and these solutions cannot be extended to the moving stage (they blow up for any finite x as $-t \to 0$).

2.3 Front velocity at start-up and restrictions on the asymptotics

We have seen that two families of self-similar solutions are available as candidates to describe different features of the asymptotics of the waiting time solutions of the problem (1), (3) close to the front and to the moment when it begins to move. Now we recall a relevant mathematical result of Aronson *et al.* (1985), that restricts the domains where the solutions of the problem (1), (3) may display a self-similar behaviour, and the kind of self-

https://doi.org/10.1017/S095679259700329X Published online by Cambridge University Press

similarity that may occur. They considered the quantity $\alpha = \lim_{x\to 0+}[x^{-2/m}h(x, -t_w)]$, and proved that: (a) if $t_w = t_\alpha \equiv t_y/\alpha^m$ ($t_y = mt_0/2\beta$, see §2.5), the initial motion of the front is due to local effects (shape of the initial profile close to $x = 0$), then $c = 0$ and $\dot{x}_f$ is continuous at $t = 0$; (b) if $t_w < t_\alpha$ the motion of the front is due to global effects (which in addition, lead to the occurrence of the corner layer), then $c \neq 0$ ($\dot{x}_f$ discontinuous at $t = 0$); in the last case, the inequality (4) holds, i.e., $|c| > c^*$. Now (if $p > 2/m$), the initial conditions (3) yield $\alpha = 0$, then $c \neq 0$. On the other hand, the LOT solutions have $c = 0$ (they satisfy $\alpha_1 \leqslant x^{-2/m}h(x, t) \leqslant \alpha_2$ for $t < 0$ and $0 < x \ll 1$). Then they cannot represent the asymptotics of the initial value problem (1), (3), for all $|t| \ll 1$ and $|x| \ll 1$. Either they are unrelated to this asymptotics, or they may yet represent it, but then, some subdomain around $t = 0$ and $x = 0$ must be excluded. The type A solutions do not suffer this limitation.

2.4 The asymptotics near start-up

Previous to the discussion of the numerical solutions and their asymptotics, let us indulge in some speculations on what to expect, and what to look for, based on theory and on intuition derived from the experiments. The crucial process in the phenomenon is clearly the development of the corner layer, as implied by the work of several authors (see, for example, Kath & Cohen, 1982; Lacey, 1983). On physical grounds, we go a step further: we believe that after a strong corner layer comes into being, it makes no difference to the phenomenon whether there is a waiting front ahead. The waiting front sitting beyond the strong corner layer is simply the foremost edge of an insignificant part of $h(x, t)$, a part that plays an irrelevant role in the evolution of the main flow behind the corner layer. In consequence, its position, and then the moment of start-up, have little (if any) practical relevance. Physically, there is a complete continuity between the strong corner layer of the last phase of the waiting stage, and the moving front after start-up. Both represent the same object, namely the leading edge of the main flow. In consequence we can regard them as a single entity (the corner layer/moving front). It stands to reason that this entity cannot display any special behavior at the moment when it overruns the front, other than merely substituting the waiting front as the foremost part of $h(x, t)$. Nothing special can happen to the velocity of the leading edge of the main flow at this moment: it cannot vanish, nor become infinite. In consequence, we expect a constant velocity asymptotics, which is equivalent to say that the velocity of the corner layer/moving front cannot change significantly in time scales $\ll t_0$ (or, equivalently, $\ll t_w$). The discontinuity of $\dot{x}_f$ at start-up and the inequality (4) are consequences of the substitution just mentioned. They state, in mathematical language, that the main flow has overrun the waiting front, and its leading edge has assumed a new name.

On the other hand, the spatial and temporal scales of the development of the corner layer, as well as its shape and velocity, must depend essentially on the global properties of $g(x)$ (its shape in the region where it is large). These in turn determine its velocity for $t \to 0$, and then, the velocity of the front at start-up. The details of $g(x)$ near the waiting front, where it is vanishingly small, cannot influence these features.

https://doi.org/10.1017/S095679259700329X Published online by Cambridge University Press

2.5 Bounds and estimates of the waiting-time and large time behaviour

Setting $V = V_B$, $Z = Z_B$ results in an exact waiting-time solution ($x > 0$) that holds for $t < 0$ (and blows-up at $t = 0$):

$$h = y(x,t) \equiv \left(-\frac{mx^2}{2\beta t}\right)^{1/m}. \tag{7}$$

Bounds of t_w can be derived (Aronson *et al.* 1983; Vázquez, 1984) comparing the initial conditions with $y(x,t)$: if two quantities $h_{0,1}, h_{0,2}$ exist, such that

$$h_{0,1} \leqslant x^{-2/m} h(x, -t_w) \leqslant h_{0,2}, \ (0 < x < x_0)$$

then $t_{y,2} \leqslant t_w \leqslant t_{y,1}$, with $t_{y,i} = mx_0^2/2\beta h_{0,i}^m$. With the initial conditions (3) and $p > 2/m$, these bounds are not very interesting if one is looking for an estimate of the waiting-time: the upper bound diverges ($t_{y,1} = \infty$), and the lower bound may not be a good approximation to t_w. We next discuss a more stringent upper bound for our initial value problem (Vázquez, 1984).

For very large times ($t \gg t_0$), the solution of the problem (1), (3) must tend to the 'point source' solution (Pattle, 1959):

$$h = s(x,t) \equiv \left[\left(\frac{mx_s'^2}{2\beta t'}\right)\left(1-\frac{x'^2}{x_s'^2}\right)\right]^{1/m}. \tag{8}$$

In (8) we have used the notation $t' = t + t_w$, $x' = x_0 - x$. The front of the point source solution is $x_s' = S^{m/\beta}\zeta_s' t'^{1/\beta}$, where $S = \int_0^{x'_P} h(x',t')\,dx'$ is proportional to the mass of the fluid per unit width of the current, and $\zeta_s' = (2\beta/m)^{1/\beta}[2\Gamma(3/2+1/m)/\sqrt{\pi}\Gamma(1+1/m)]^{-m/\beta}$ ($\zeta_s' \cong 1.411\ldots$ for $m = 3$). The self-similar solution (8) corresponds to the initial condition $g(x) = 2S\delta(x')$ and describes the asymptotics of any problem in which g is localized near x_0, independently of the details of the initial profile. The front of $s(x,t)$ arrives at the position of the waiting front ($x = 0$) at $t' = t_s'(m) \equiv (x_0/\zeta_s')^\beta S^{-m}$ ($t_s'(3) = 0.1786\ldots \times x_0^5/S^3$). For the initial conditions (3) and $p \gg 1$, it is reasonable to expect that t_w will be close to t_s' (calculated with the appropriate S). In general, t_s' is an upper bound of the waiting-time, $t_w < t_s'$, and may give in many instances a better estimate than $t_{y,1}$. Actually, experiments on viscous gravity currents (Gratton *et al.*, 1992) have shown that t_s' is a good approximation of t_w for $p \approx 1$. This is confirmed by the numerical calculations. The most unfavourable case occurs for $p = 2/m$. For example, for $m = 3$, $p = 2/3$ one finds $t_w = 0.0648$ (in units of x_0^5/S^3), which differs considerably from $t_s'(3)$, but is of the same order of magnitude.

3 Numerical solutions

3.1 Method and details of calculations

We solve the problem (1), (3) for the case of viscous gravity currents, and for various values of p. We do the calculations in terms of t' since t_w is yet unknown. We employ the dimensionless variables $\tilde{h} = h/h_0$; $\tilde{x} = x/x_0$; $\tilde{t}/t_0$; $\tilde{u} = u/u_0$ (x_0: the initial length of the current, $h_0 \equiv g(x_0)$, $t_0 \equiv x_0^2/h_0^3$, $u_0 \equiv h_0^3/x_0$), then the equation to be solved is ($m = 3$):

$$\tilde{h}_{\tilde{t}'} = (\tilde{h}^3 \tilde{h}_{\tilde{x}})_{\tilde{x}} \tag{9}$$

We assume $\tilde{g}(\tilde{x}) = (p+1)\tilde{x}^p$ ($p > 0$) for $0 \leqslant \tilde{x} \leqslant 1$ and $\tilde{g}(\tilde{x}) = 0$ for $\tilde{x} < 0$ (then $S = 1$). At

https://doi.org/10.1017/S095679259700329X Published online by Cambridge University Press

$\tilde{x} = 1$ there is an ideal wall that supports the fluid (in the following we shall omit the tildes as no confusion will arise). To discretize (9) we employ a three-level second order finite difference implicit scheme, centred in time and space. For each time step we derive a system of algebraic equations and solve it by iterations with the Gauss–Seidel nonlinear inversion method. The code includes a correction process that accelerates the iterations by using a less stringent convergence criterion (Hirt & Harlow, 1967). We denote the time and grid points where we calculate the quantities by superscripts and subscripts, respectively. The grid has $2N+1$ points and is non-uniform to achieve good accuracy near $x = 0$ with N not too large for the computation (Kálnay de Rivas, 1972). To this end we set $x_j = \xi_j|\xi_j|$, $-1 \leqslant \xi_j \leqslant 1$ with $\Delta\xi = 1/N$. Then $h_{t'}^{n+1} \approx (3h^{n+1} - 4h^n + h^{n-1})/2\Delta t'$, with an error $O(\Delta t'^2)$. To conserve S better we discretize the right-hand side of (9) as:

$$[(h^3 h_x)_x]_j^{n'} \approx \Delta x^{-2}\{(h^3)_{j+1/2}^{n'}(h_{j+1}^{n'} - h_j^{n'}) - (h^3)_{j-1/2}^{n'}(h_j^{n'} - h_{j-1}^{n'})\}\,(n' = n+1).$$

In this way we obtain the tridiagonal system ($j = 2, 3, \ldots, 2N$):

$$\tfrac{3}{2}h_j^{n+1} - \mu(a_j^{n+1}h_{j-1}^{n+1} - b_j^{n+1}h_j^{n+1} + c_j^{n+1}h_{j+1}^{n+1}) = 2h_j^n - \tfrac{1}{2}h_j^{n-1}, \tag{10}$$

in which $\mu = \Delta t'/\Delta x^2$; $a_j^s = (h^3)_{j-1/2}^s \equiv \frac{1}{2}[h_j^3 + h_{j-1}^3]^s$; $c_j^s = (h^3)_{j+1/2}^s \equiv \frac{1}{2}[h_{j+1}^3 + h_k^3]^s$; $b_j^s = a_j^s + c_j^s$.

The boundary condition $h_x = 0$ at the wall ($j = 1$) gives $(h_2 - h_0)/2\Delta x = 0$, then $h_2 = h_0$ and $c_1^n = a_1^n$, and the equation for this node is $(\frac{3}{2} + \lambda b_1^{n+1})h_1^{n+1} - 2\lambda c_1^{n+1}h_2^{n+1} = 2h_1^n - \frac{1}{2}h_1^{n-1}$. In the last point of the grid ($j = 2N+1$), where always $h = 0$) we require $h_{2N+1} = 0$.

The error of the approximation for $h_{t'}$ is $\epsilon \approx 653(\bar{h}^2/\bar{x})^6\,\Delta t'^2$ ($\bar{x} \cong 1$ and $\bar{h} \cong 1$ are the scales of x and h) then $\epsilon \ll 1$ determines $\Delta t'$. With these choices and $N \approx 10^3$ the numerical scheme is unconditionally stable and the results are satisfactory for our purposes. The mass is conserved to an approximation better than one part in $\approx 10^6$.

A few additional comments are in order concerning the accuracy of the calculations. In general, due to the discretization, numerical methods will not yield a good approximation to the exact solution in those regions where h_x changes very rapidly (from one grid point to the next), as occurs near the leading edge of a strong corner layer and very close to an advancing front. Moreover, our non-uniform grid will produce spurious effects. Consider, for example, what happens if we try to reproduce with our numerical scheme the constant velocity solution (6), that is an exact solution of (1). The front of the numerical solution will be distorted with respect to the true solution, since there h_x changes very rapidly. The magnitude of the distortion depends on the local density of the grid points. Since the grid is not uniform, the distortion will vary as the front travels and passes through regions where the grid spacing is different. The consequences of this change in the shape is that the velocity of the front of the numerical solution will vary as the front moves. This spurious effect will be larger when the front passes through $x = 0$, where the spacings vary very rapidly. The spurious effects just discussed will also be present in our numerical solutions of (1), (3), and will be especially relevant when the corner layer is arriving at $x = 0$, and when the front starts moving. Fortunately, this drawback does not invalidate our numerical method. As we shall see, there is a device that allows to recover the information we want, but we must be very careful in the interpretation of the results. In fact, we can recognize and subtract the spurious effects, by comparing calculations with different N (see more details below). With this purpose we have computed solutions with $N = 1000$ and 4000 to find the true asymptotics close to start-up. In domains not too close to the corner layer or

https://doi.org/10.1017/S095679259700329X Published online by Cambridge University Press

the front, and then, not too close to start-up, the comparison of the results obtained with the coarser and finer grid show insignificant differences, indicating that they are free of spurious effects. For practical reasons we made these verifications only for $p = 1$. In the calculations for $p \neq 1$ we only employ $N = 1000$, since we can use the results for $p = 1$ as a guide to interpret the solutions unambiguously.

We follow the evolution of each solution until the front starts to move and travels a distance of the order of unity. Having found t_w we compute $t^n = t'^n - t_w$. A good accuracy ($\epsilon \approx 10^{-5}$) requires short time steps: $\Delta t' \approx 10^{-6}$ ($N = 1000$) and $\Delta t' \approx 10^{-8}$ ($N = 4000$), which imply long computations. We used an Apollo 750 workstation (≈ 40 Mflops) and the graphical package Starbase™ to visualize the solution in real time. Each $N = 1000$ and $N = 4000$ solution took about 4 and 70 hours to run, respectively.

To achieve a reliable test of the asymptotics we need a very accurate determination of t_w, which in turn depends on the criterion we employ to decide when the front starts moving. Clearly it is not legitimate to find t_w extrapolating the numerical law of motion of the front, since this implies to assume *a priori* a specific law of motion in the limit $|t| \to 0$. We tested several criteria, based on the observation of the first grid point ahead of the waiting front ($x_N = -1/N^2$): (a) the arrival of fluid (we arbitrarily fixed a bound $\Delta = 10^{-8}$; if $h_N > \Delta$ we assume that the front has moved, since fluid has arrived in the region $x < 0$); (b) the onset of a significant flow velocity u_N at x_N; (c) the onset of a significant mass flow $h_N u_N$ at x_N. These criteria yield always consistent and unambiguous results (the front motion 'begins' at the same time step, while sudden jumps of several orders of magnitude of h_N, u_N and $h_N u_N$ occur at this moment), and then we finally decided to use (a). We can safely assume that the uncertainty of the numerical t_w is of the order of $\Delta t'$. Of course, the true t_w may differ from the numerical t_w by a larger amount, due to the accumulation of errors of the numerical method. This difference is unknown, but certainly small (the t_w obtained with the $N = 1000$ and $N = 4000$ calculations differ by less than 0.007%). In a similar way, we determine the position of the front by means of a $h_j > \Delta$ criterion. We define (arbitrarily) the 'position' of the corner layer as the place where h_x is maximum.

3.2 Methods of analysis

We have considered various methods to determine when and where the asymptotics of the numerical solution is self-similar and to find the corresponding exponent δ. They involve certain elaborations of the numerical results and their reliability depends on the type of data employed. The present discussion will help to appraise the significance of the results we report in the next section. The methods use: (a) the profile at $t' = t_w$; (b) the motion of the corner layer and the front; (c) the profile for times close to start-up.

The basis of method (a) is that at start-up the self-similar solutions of (1) have the simple form:

$$h = z_\infty x^{(2-1/\delta)/m}, \quad u = u_\infty x^{1-1/\delta}, \tag{11}$$

with $\delta > 1$ for the LOT solutions and $\delta \leqslant 1$ for the A solutions with

$$z_\infty = \lim_{\zeta \to \infty} (b\zeta)^{1/m\delta} Z^{1/m}, \quad u_\infty = \lim_{\zeta \to \infty} (b\zeta)^{1/\delta} V.$$

For the theoretical reasons discussed previously, we expect that the numerical solution may

https://doi.org/10.1017/S095679259700329X Published online by Cambridge University Press

display the power law behaviour (11) with $\delta > 1$ in some interval $\epsilon_1 x_0 < x < \epsilon_2 x_0$, ($\epsilon_1 \ll \epsilon_2 \ll 1$), and eventually, with $\delta \leqslant 1$ in some other interval $0 < x < \epsilon_1 x_0$. If either of these expectations is fulfilled (or both), we can determine the corresponding δ by means (say) of a linear fit (in the appropriate interval) of a $\log(h)$ vs. $\log(x)$ plot. To this purpose we employ the following criterion: let $R(x) = h(x,0)/x^{(2-1/\delta)/3}$, and let $\epsilon_a > 0$ be the desired margin of tolerance (we usually set $\epsilon_a \approx 10^{-3}$ or less); then if an interval $x_1 \leqslant x \leqslant x_2$ exists, such that $K \leqslant R(x) \leqslant K + \epsilon_a$, where K is a constant, we say that (within the margin of tolerance ϵ_a) the numerical solution has a self-similar behavior in the said interval. Notice that we do not know in advance the location of the interval involved. Also, its extent depends on ϵ_a. In using this method we must keep in mind that t_w has an uncertainty $O(\Delta t')$, that due to the spatial discretization, the numerical scheme cannot yield a good approximation to the exact $h(x,0)$ very close to $x = 0$, and that there are spurious effects due to the non uniformity of the grid. For these reasons we must be careful when considering the grid points close to the front. With these qualifications, this method has the advantage that it depends on the behavior of the numerical solution in a domain where it is a reliable approximation of the true solution.

The method (b) uses the fact that $x_c, x_f \propto t^\delta$ for the self-similar solutions, so that we expect that the numerical solution will tend to this asymptotics for $|t| \ll t_w$. To decide if and when the numerical data display self-similarity, we use a tolerance criterion similar to that described above. We must be careful when using this method, in particular when considering the motion of the corner layer. It is very sensitive to the uncertainty of t_w, and it depends critically on how we defined the position of the corner layer. In addition, if p is close to 2/3, a well-defined corner layer appears only just before the end of the waiting-time stage, and very near to $x = 0$, so that it is difficult to determine accurately its law of motion. A further drawback is that the accuracy of the position of the corner layer (defined by $h_{xx}(x_c) = 0$) depends on the numerical solution in the region where it is less reliable for the reasons already discussed. These problems increase as $t' \to t_w$, precisely the limit we want to study.

For any self-similar solution of (1) the relation

$$h^3 t/x^2 = Z(x/bt^\delta) = \tilde{Z}(x/t^\delta) \tag{12}$$

holds, in which $\tilde{Z}$ is a function that depends on δ and the type of self-similarity. This is used to study the profile for $t' \to t_w$. The method (c) consists in comparing graphs of the numerical values of $h^3 t/x^2$ vs. x/t^δ of a given run, for different t. By choosing a suitable δ, we can achieve an accurate overlap of the graphs in the domains where the numerical solution is self-similar (it is convenient to show the graphs in logarithmic scale). In the same process we can make comparisons with the self-similar solutions of type LOT or A, to find the domains where these asymptotics apply. This method is important because it allows a direct comparison between the numerical solution and the exact self-similar solutions. The test is very stringent because we use a single parameter (δ) to fit a series of curves corresponding to different t. However it is painstaking to achieve the optimum fit. In addition it will turn out (see below) that δ is always close to unity, and then the quality of the fit is rather insensitive to the small changes in δ involved. Method (c) is not practical if one only want to find δ, and we used it only to check consistency with the δ obtained by other methods.

A moving front has the property that $\dot{x}_f(t) \approx -\lim_{x \to x_f} h^3/3(x-x_f)$, $x > x_f$. Then one might hope to find the velocity of the front by studying the profile of the numerical solution very close to it. The same procedure could allow to find the velocity of a strong corner layer overtaking a vanishingly thin film of fluid, as occurs near the end of the waiting-time stage. The method looks attractive, since it does not depend on the accuracy of t_w nor on any assumption about self-similarity. Unfortunately, it depends on the value of $h(x, t)$ at the grid points where the numerical solution is unreliable. It is impossible to overcome this flaw. In consequence no useful additional information can be gained with this method.

To sum up this discussion we can say that the more reliable deteminations of δ and of the kind of self-similarity are obtained with method (a), complemented by method (c) to test how well the self-similar solutions fit the numerical calculations. The law of motion (method (b)) of the corner layer and the moving front is less reliable regarding the asymptotics close to $t = 0$; but can be used to check consistency with the results of the other methods. In all cases, we must be careful to exclude spurious numerical effects.

4 Numerical results ($m = 3$)

4.1 General properties of the solutions for power law initial profiles

The front of the numerical solutions for $0 < p < 2/3$ starts moving immediately ($t_w = 0$). We shall not comment further these cases, but shall discuss in detail the solutions for $p > 2/3$, that have non-vanishing waiting-times. In all these solutions a single corner layer develops. In Figure 2, we give an example that displays the typical behavior of our waiting-time solutions. As soon as the process begins, the profile changes and we can recognize two domains, separated by a moving transition interval. The transition occurs around an intermediate position $x_c(t')$, defined as the point where h_x attains its maximum h_{xM}. In the domain near the wall ($x_c < x < 1$) the profile differs markedly from its initial shape and $h_{xx} < 0$ (h_x increases monotonically as one goes from the wall, where it vanishes, to x_c). In the domain near the front ($0 < x < x_c$) the profile changes very little from the initial shape and $h_{xx} > 0$ (h_x increases monotonically as one goes from the front to x_c). The transition is characterized by large changes of h_x and h_{xx}. While it travels towards the front, its width reduces, and h_{xM} and the amplitude of the oscillation of h_{xx} increase. Late during the waiting stage the transition can be appropriately described as a corner layer. The development of the corner layer is a gradual process, so that there is no particular time in which the corner layer begins to exist. To describe the time scale and location of this process, avoiding unnecessarily long circumlocutions, it is convenient to introduce some notation and terminology. We call 'time of formation' of the corner layer the time t_{c0} when h_{xM} exceeds a bound (arbitrarily chosen) and 'place of formation' x_{c0} the position of h_{xM} when this happens ($x_{c0} = x_c(t' = t_{c0})$). Specifically, we define t_{c0} by

$$h_{xM}(t' = t_{c0}) = 10p(p+1)\, x_c^{p-1}.$$

In all the numerical solutions with $p > 2/3$ we find $0 < t_{c0} < t_w$, and $0 < x_{c0} < 1$. As the corner layer travels, it becomes progressively narrower and stronger, and becomes a corner shock precisely when it catches up with the front. When this happens, the front begins to move. The time and place of formation of the corner layer depend on p. It forms earlier and nearer to the wall for p very large, and as $p \to 2/3$ the time $t_{c0} \to t_w$ and $x_{c0} \to 0$.

https://doi.org/10.1017/S095679259700329X Published online by Cambridge University Press

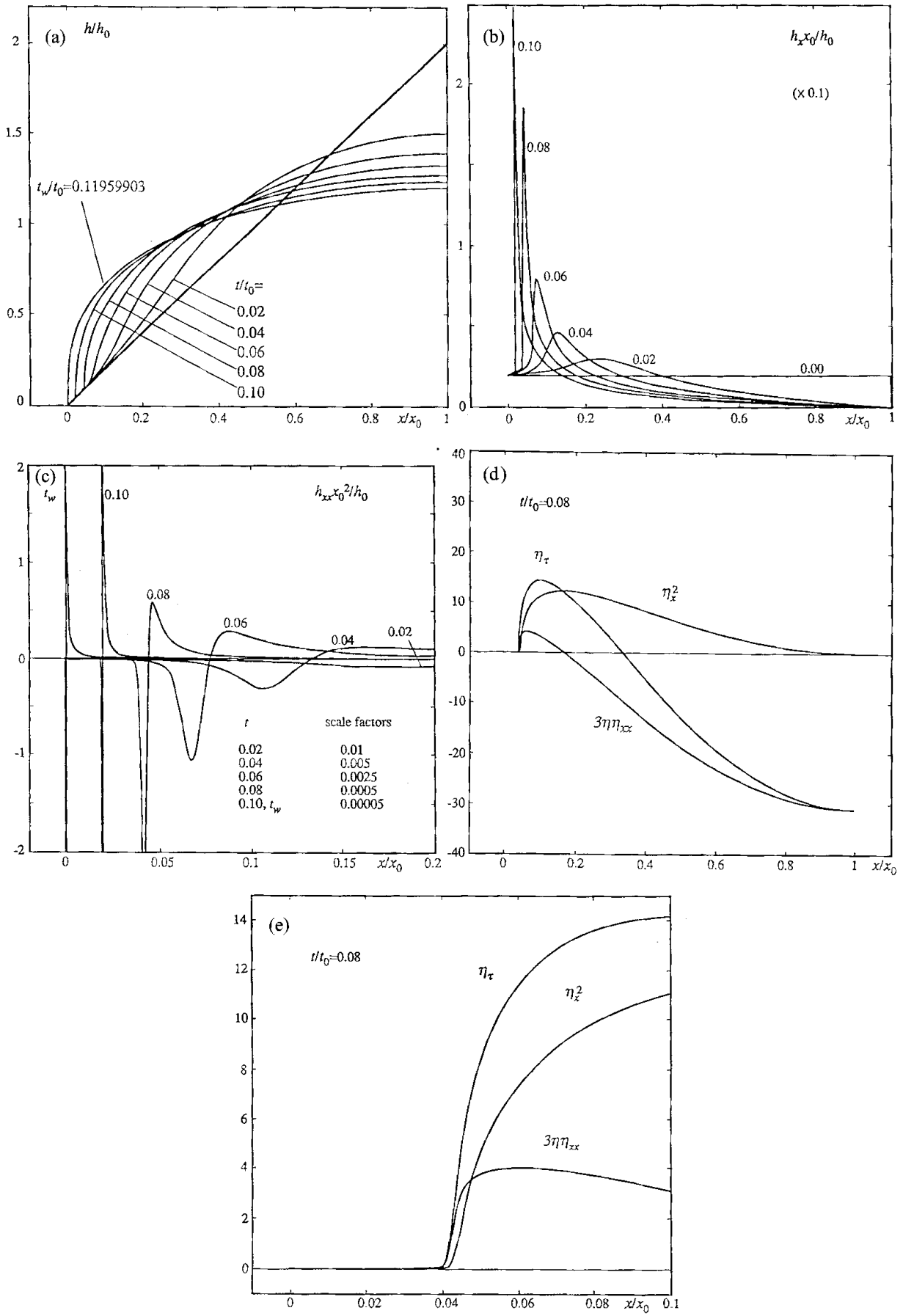

FIGURE 2. Numerical solution ($p = 1$) during the waiting stage: (a)–(c) evolution of $\tilde{h}$, $\tilde{h}_x$ and $\tilde{h}_{xx}$; (d), (e) nonlinear propagation and diffusion terms.

https://doi.org/10.1017/S095679259700329X Published online by Cambridge University Press

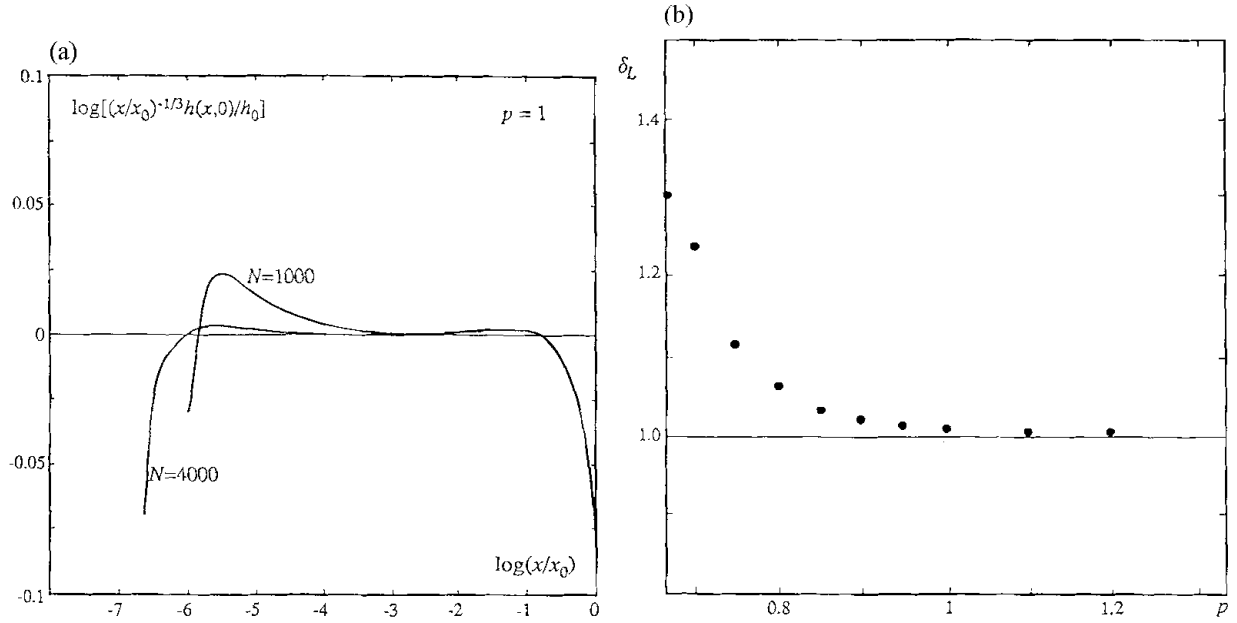

FIGURE 3. Self-similar asymptotics of the numerical solutions (a) profile at start-up: $\log[x^{-1/3}h(x,0)]$ vs. $\log x$ ($p = 1$); (b) self-similarity exponent $\delta_L(p)$.

In Figures 2d and 2e, we plot the different terms of (2) for a numerical solution ($p = 1$) at two different times during the waiting stage. There are four domains where different behaviors are displayed: (a) near the wall, the diffusion term $m\eta\eta_{xx}$ dominates; (b) in an intermediate region, far from the wall but behind the corner layer, the nonlinear term η_x^2 prevails; (c) in a very small region around the corner layer, the diffusion term dominates again; and (d) in the region ahead of the corner layer, both terms (and then η_t) are extremely small. The regions (b) and (c) roughly correspond to the two domains where different self-similar asymptotics develop, as will be discussed below.

The behavior of our numerical solutions is in accord with theory. It also agrees very well (subtracting the two-dimensional and surface tension effects) with accurate experiments on the spreading of linear ramps of viscous liquids (Marino *et al.*, 1995), and with other numerical solutions (Del Carmen & Ferreri, 1995; Marino *et al.*, 1995).

After start-up the qualitative behavior of the numerical solutions is very simple, and in accord to what is expected for a moving front. For very large t', the self-similar point source solution is closely approached.

4.2 The asymptotics close to the front and start-up

The profile at start-up $h(x,0)$ (method (a)) displays *two* self-similar regimes. We arrive at this conclusion after the following analysis. In Figure 3a we plot $\log[x^{-1/3}h(x,0)]$ vs. $\log(x)$ for the $p = 1$ numerical solutions with $N = 1000$ and 4000. This presentation has the advantage that a self-similar behavior with $\delta = 1$ appears as a horizontal line, and positive or negative slopes correspond to $\delta > 1$ or $\delta < 1$, respectively. We see that both solutions coincide exactly, except very close to the front where the plots curve upwards (apparently suggesting $\delta < 1$). The curving up occurs near $x \approx 10^{-3}x_0$ for the $N = 1000$ solution and $x \approx 10^{-4}x_0$ for $N = 4000$. This different behavior brands the curving-up as a spurious effect due to the non uniform grid, that distorts the profile for small x ($x < 10^{-3}x_0$ for the $N = 1000$ solution and $x < 10^{-4}x_0$ for $N = 4000$). It is sensible to assume that the effect: (a)

https://doi.org/10.1017/S095679259700329X Published online by Cambridge University Press

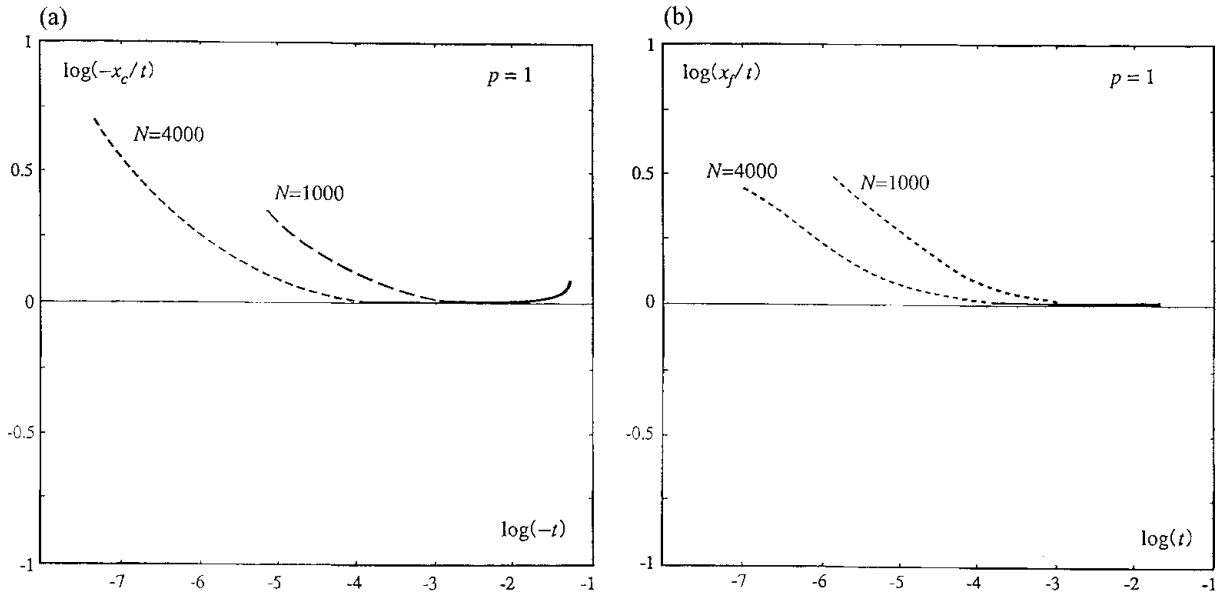

FIGURE 4. Motion of the corner layer and of the front: (a) $\log(-x_c/t)$ vs. $\log(-t)$; (b) $\log(x_f/t)$ vs. $\log(t)$. Both graphs correspond to $p = 1$.

depends on N, (b) as N is increased its onset occurs for smaller x, (c) as N is varied, it only changes its scale. This is precisely what we see in Figure 3a, and it allows to find the domain in which the numerical solution is free of the spurious effect. Where the $N = 1000$ and $N = 4000$ solutions overlap accurately, we can guarantee that the $N = 1000$ solution is free from a significant spurious effect (and *a fortiori*, the same is true for the $N = 4000$ solution). This we conclude that the straight (very short) horizontal part of the $N = 1000$ graph is a genuine result (i.e. it represents the behavior of the true solution). We also conclude that the longer (more than one decade in length) horizontal part of the $N = 4000$ graph is a genuine result, because we know that the fraction that overlaps the $N = 1000$ graph is genuine, and the rest must also be genuine, as follows from the scaling property of the spurious effect. By the same arguments, we conclude that a calculation with a sufficiently large N should produce a graph with a straight horizontal part that extends to any arbitrarily small value of x. Then we infer that the small x behavior of the true solution is of type A, with $\delta = 1$, i.e. it is described by a constant velocity front solution $w(x, t)$ (6).

In Figure 3a we also observe an intermediate range, still far from the wall $\epsilon_x x_0 \ll x \ll x_0$ ($\epsilon_x \approx 5 \times 10^{-3} x_0$ for $p = 1$), in which the behavior is of type L (with $\delta = \delta_L$ larger, but close, to unity). In this range both numerical calculations coincide, and we can safely assume that no spurious numerical effect is present.

Similar results are obtained (with $N = 1000$) for any $p > 2/3$, with $\delta_A = 1$ (as inferred from the presence of a small horizontal part in the $\log[x^{-1/3} h(x, 0)]$ vs. $\log(x)$ graphs), and $\delta_L = \delta_L(p)$. In Figure 3b we represent the $\delta_L(p)$ obtained by this method, showing that $1 < \delta_L(p) < 13/10$, with $\delta_L \to 13/10$ for $p \to 2/3$ and $\delta_L \to 1$ for $p \to \infty$.

The laws of motion of the corner layer (during the waiting stage) and of the front (during the moving stage) are shown in Figure 4, in which we plot $\log(-x_c/t)$ and $\log(x_f/t)$ vs. $\log(|t|)$ for the numerical solutions for $p = 1$, and $N = 1000, 4000$. The comparison of the high and low spatial resolution results indicates that the curving up that occurs in both graphs to the left of $t \approx 10^{-3} t_w$ for the $N = 1000$ solution and $t \approx 10^{-4} t_w$ for $N = 4000$ is due to the spurious numerical effect, already discussed in connection with the profile at

https://doi.org/10.1017/S095679259700329X Published online by Cambridge University Press

start-up. By means of the argument then used, we can subtract the effect. In consequence we infer that the true velocity of the corner layer and of the front tends to the same constant value $c \neq 0$ in the limit $|t| \to 0$. This means that the motion of the corner layer joins smoothly at start-up with the motion of the front, and it is consistent with a $\delta = 1$ type A asymptotics as already obtained using method (a). Coming back to the motion of the corner layer, Figure 4a shows that there is a time interval $\epsilon_t t_w < |t| \ll t_w$ ($\epsilon_t \ll 1$, for example $\epsilon_t \approx 10^{-2}$ for $p = 1$) that excludes the neighborhood of $t = 0$, in which $x_{cl} \propto |t|^{\delta_L}$ with $1 < \delta_L(p) < 13/10$. Then in this interval the motion follows a type L behaviour. In this range no spurious numerical effect occurs (as shown by the coincidence of the $N = 1000$ and 4000 results), and the method (b) allows to determine $\delta_L(p)$, in good agreement with that obtained from the intermediate region of the profile at start-up.

We have used the self-similarity exponents δ_L and $\delta_A = 1$ obtained by method (a) to compare the profiles $h(x, t)$ for different times during the waiting-time stage with the appropriate L ($h_L(x, t)$) and constant velocity front ($w(x, t)$) solutions (method (c)). Since the procedure is cumbersome, we only considered the case $p = 1$. In Figure 5a we have represented $\log[(t/x^2)^{1/3} h(x, t)]$ vs. $\Lambda = \log(x/t^{\delta_L})$ for a series of t, near the end of the waiting stage ($-0.7 \times t_w < t < 0$, when the corner layer, that appears at $\Lambda \approx 0$, has already developed). The details of the evolution of the profile reveal some subtle features. The first profile of the series has already approached the L solution, but only in a small domain $0 < \Lambda < \Lambda_L(t)$ not far behind the corner layer. As t increases, Λ_L grows, and the domain in which the numerical solution approaches the L solution expands. However, studying carefully the graphs, we notice that very close to the corner layer a small subdomain $0 < \Lambda < \Lambda_A(t)$ ($\Lambda_A(t) \ll \Lambda_L(t)$) appears and enlarges as $t \to 0$. In this subdomain the behavior of the numerical solution is not well represented by the L solution (the departures increase as $t \to 0$), and the A solution gives a better approximation (see Figures 5b, c). In consequence, during the last phase of the waiting-time stage there are two regions of self-similarity: the region $0 < \Lambda < \Lambda_A(t)$ just behind the corner layer (type A, constant velocity) and the intermediate region $\Lambda_A(t) < \Lambda < \Lambda_L(t)$ (type L). The accuracy with which the L solution describes the asymptotics in this domain is impressive. In the region close to the corner layer the constant velocity solution gives a very good description of the asymptotics (except very close to the corner layer, where the numerical solution departs from the true solution due to the spurious effects we have already discussed). These domains correspond to those observed in the profile at start-up. The peculiar behavior of the profile is consistent with the observations of the motion of the corner layer: as long as $\Lambda_A(t)$ remains small (i.e. t is not too close to 0), the motion is very approximately of type L, but as start-up is approached it tends to the constant velocity solution.

To complete the discussion of the numerical profiles, we notice that (as expected) in the domain near the wall ($\Lambda > \Lambda_L(t)$) there is no self-similar behavior, and that ahead of the corner layer ($\Lambda < 0$) only very small changes with respect to the initial profile occur.

Summarizing, an asymptotics of type L appears in an intermediate domain near and behind the corner layer, and a constant velocity asymptotics (type A) develops very close to the corner layer during the last phase of the waiting stage. Asymptotics of type S and N are never observed. Only parts of the full L and A solutions describe the asymptotics of the numerical solutions: a piece of the L solution behind the first corner shock of the series, and a small portion of the A solution just behind the front. This is a consequence of our choice of initial conditions, as will be discussed below.

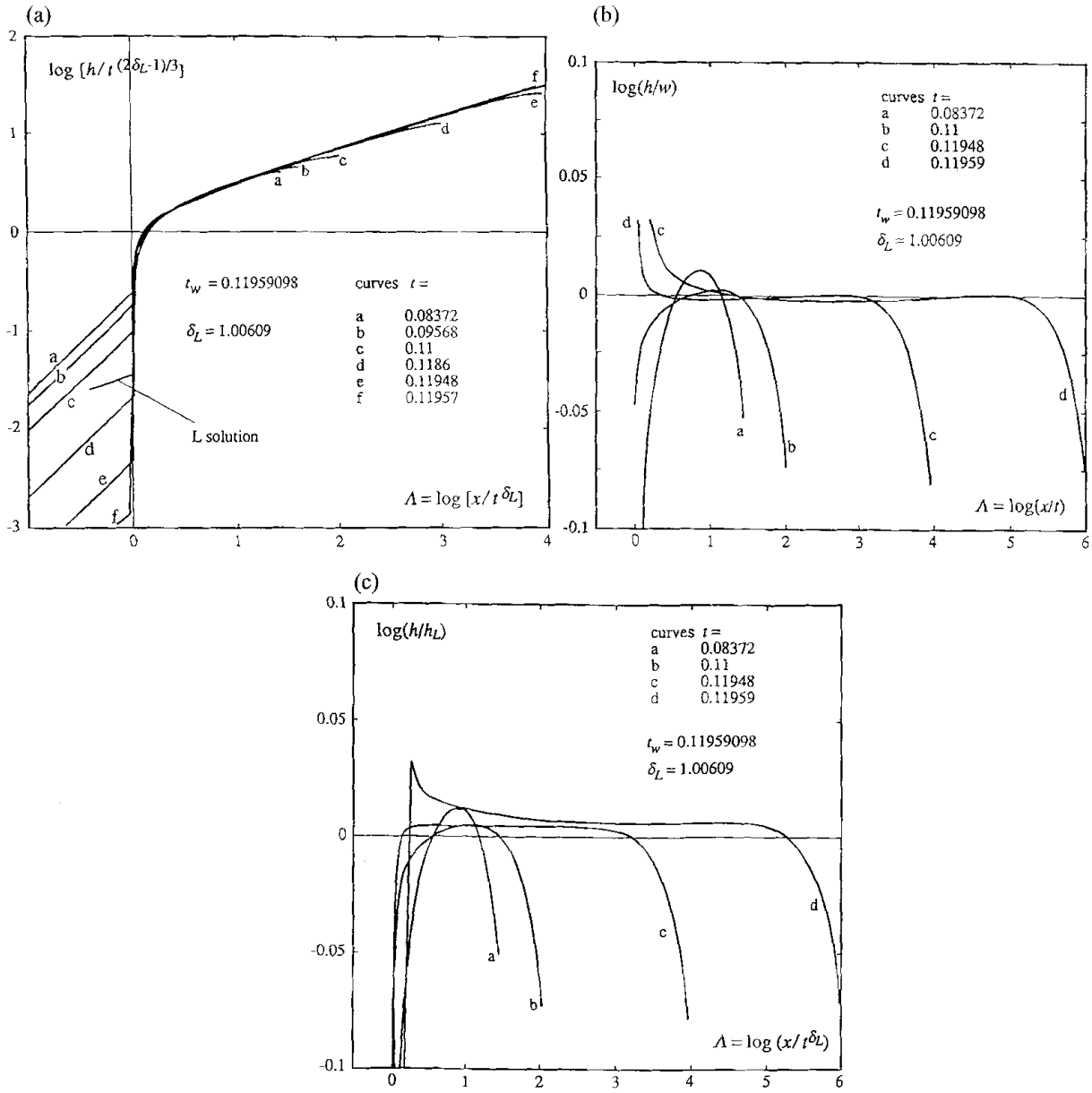

FIGURE 5. Self-similarity during the waiting stage ($p = 1$) as start-up is approached: (a) $\log[h/t^{(2\delta_L-1)/3}]$ vs. $\log(x/t^{\delta_L})$, showing how the solution approaches to the type L self-similarity in the intermediate region; (b) $\log[h/w]$ vs. $\log(x/t)$ and (c) $\log[h/h_L]$ vs. $\log(x/t^{\delta_L})$, showing how the solution approaches to the constant velocity solution close to the corner layer, but at the same time maintains the type L self-similarity in the intermediate region.

4.3 Front velocity at start-up

On the basis of the profiles at start-up and at previous times, as well as on the motion of the front (and discounting spurious numerical effects), we have concluded that a type A asymptotics with $\delta_A = 1$ holds near the front, which means $c = \dot{x}_f(t = 0+) \neq 0$ as predicted by theory. The absolute value of the start-up velocity is an increasing function of p, and can be determined from our numerical solutions using method (b), or equivalently by method (a). For $p = 1$, the extrapolation of the first reliable numerical values of $\dot{x}_f$ (corresponding to t close to $\approx 10^{-2} t_w$ for the $N = 1000$ solution and $\approx 10^{-3} t_w$ for $N = 4000$) yields $|c|t_0/x_0 \approx 1$, that exceeds $1/144$ (the lower bound given by (4) for $m = 3$) by more of two orders of magnitude. For $p \to \infty$, when the solution tends to $s(x, t)$, we find

https://doi.org/10.1017/S095679259700329X Published online by Cambridge University Press

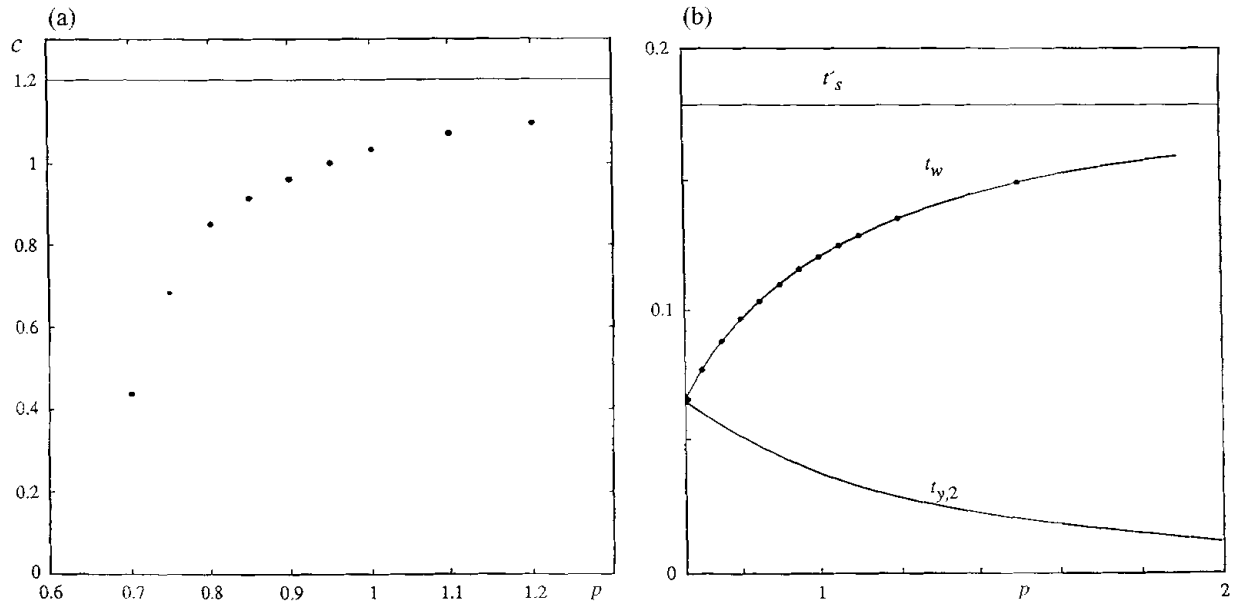

FIGURE 6. (a) Velocity of the front after start-up. (b) waiting-time $t_w(p)$.

$|c|t_0/x_0 \to \zeta_s'^5/5 \approx 1.2$. This yields a theoretical upper bound of c: $|c| \leqslant \zeta_s'^5 x_0/5t_0 \approx 1.2x_0/t_0$. Other values are shown in Figure 6a. Our numerical investigation does not permit to find c when p is very close to 2/3 (the difficulty in resolving the domain where the constant velocity asymptotics occurs becomes insurmountable when $p \to 2/3$). We conclude that the lower bound (4) does not give a practical estimate of the velocity at start-up, at least for p not very close to 2/3.

For ($t' > t_w$), a practical estimate (by excess) of $\dot{x}_f$ is given by the velocity of the front of the point source solution (5), i.e. $\dot{x}_s(t') = S^{3/5}\zeta_s' t'^{-4/5}/5$ (see Figure 6a). The velocity of the corner layer and of the front of a type L solution vanish at $t = 0$, but this does not contradict (4), since the L solution only describes the asymptotics of the numerical solution in the intermediate region, that does not include $x = 0$ and $t = 0$.

4.4 Magnitude of the waiting-time and large-time behaviour

We plot the numerical values of t_w in Figure 6b, where we also show the lower and upper bounds $t_{y,2}$ and t'_s (for $S = 1$). As expected t'_s is a reasonably good practical estimate (by excess) of t_w, for large p. On the contrary, $t_w \gg t_{y,2}$, except for p very close to 2/3. The quantity $l_0 = 1 - 2^{-1/(p+1)}$ gives a measure of the concentration of the initial distribution of fluid (half of the fluid is initially in the interval $(1-l_0)x_0 < x < x_0$). If $p \to \infty$, $l_0 \to 0$, and all the fluid is concentrated at x_0. In this limit the point source solution is an exact solution of our initial value problem, then $\lim_{p\to\infty} t_w = t'_s$. The smaller is p, the less is the concentration of the initial condition, then the waiting-time is shorter, and the estimate given by t'_s impairs (Figure 6b). It is interesting to observe that the numerical solution approaches rapidly the point source solution: for $t' \approx 2t_w$ the difference is already small. For many practical purposes the point source solution is a good approximation in the moving stage (as observed by Gratton *et al.*, 1992, for $p = 1$).

https://doi.org/10.1017/S095679259700329X Published online by Cambridge University Press

5 Discussion

In any problem of physical interest (defined in a bounded support), an arbitrary initial profile with a front at $x = 0$ will have a dominant term of the form x^p for $x \to 0$. If $0 < p < 2/3$, the front moves at once. If $p > 2/3$, a corner layer appears before start-up. Then any waiting time solution of practical interest develops at least one corner layer (an exception occurs if the initial profile coincides everywhere with the singular solution (7), then no corner layer appears during the waiting stage). In consequence, we conclude that no conceivable initial condition will tend to asymptotics of type S or N (that do not display corner layers). This may be related to the instability of these self-similar solutions. We have performed a stability analysis (unpublished) of the phase plane using the Lyapunov functional approach, and proved that the integral curves in the neighbourhood of the singular point B are unstable, which implies that the parts of the self-similar solutions represented by integral curves approaching B cannot be attractors.

We were puzzled to find that when the numerical solution approaches a type L asymptotics only one corner layer appears (the first of the series). We ascertained that this is a consequence of our initial conditions, and not an artifact of the numerical method. This suspicion arises because the subsequent corner layers of the L solutions appear in scales that decrease geometrically, which makes very difficult, perhaps impossible, to detect them in the solutions. To discard this possibility we have made two tests: (a) we tried other numerical schemes specifically devised to achieve high resolution in the domain of interest, and we always obtained a single corner layer in solutions with the initial conditions (3), (b) we computed the evolution of an initial condition consisting of a piece of a type L profile (with two corner layers), and found that the numerical solution preserves both corner layers, which remain observable during the waiting stage. Then we conclude that the occurrence of a single corner layer is a true property of our waiting-time solutions. This peculiar behavior can be explained heuristically, observing that (according to (1)) the time scale for profile modifications is $T \approx |h/h_t| \approx L^2/h^3$, where L is the spatial scale of variation of h. With a power-law initial profile, $T(x) \propto x^{-3p}$. Then near $x = 0$ (and ahead of the first corner layer) the profile changes very slowly ($T(x) \gg t_w$ for $x \ll 1$). In consequence the first corner layer arrives to the front (ending the waiting stage) too rapidly for the subsequent ones to develop. This is why only part of the L solution plays a role in the asymptotics of our problem. However, the rest of this self-similar solution is also physically meaningful, and plays a role in the asymptotics of different initial value problems, as proved by the example (b) above.

More peculiar yet is the fact that the solution tends to different self-similarities in two regions: type L in an intermediate region that excludes a neighborhood of the front (the motion of the corner layer is also of type L for $|t| \ll t_w$, but excluding the vicinity of $t = 0$), and of constant velocity very close to the front and of $t = 0$ (the A solutions with $\delta < 1$ do not play any role in this asymptotics, as is suggested by their blowing-up behavior at start-up). This remarkable behavior reconciles the occurrence of a type L asymptotics with the discontinuity of the front velocity at start-up. We have not yet found a rigorous theoretical explanation of why the evolution of the solution follows such an intricate path, but as discussed in §2.4, the crucial point is the development of the corner layer. Loosely speaking, the evolution of the solution occurs in two steps. During most of the waiting

stage, from the beginning of the phenomenon until there is a well-defined corner layer, the shape of the solution in the domain near the front $0 < x < x_c$ is still relevant, and influences the phenomenon everywhere ($0 < x < x_0$). In this phase the initial condition forces the solution to approach a self-similar asymptotics of type L with a certain $\delta_L(p)$ (determined by the global initial profile), and then to develop a corner layer. As the end of the waiting stage is approached, the main flow (i.e. the solution behind the increasingly strong corner layer) dominates the process, and the state of the flow downstream ($0 < x < x_c$) has a vanishingly small influence on the solution upstream ($x_c < x < x_0$). In this phase, the solution close to, and behind the corner layer, becomes independent on the solution in the downstream domain. In other words, the existence of the waiting front becomes irrelevant for the main flow ($x_c < x < x_0$), which to all practical purposes evolves as if there were nothing ahead. Then it cannot follow the L solution, but tends to the constant velocity asymptotics. The resulting $\delta_A = 1$ is not related to the shape of the initial profile near the front. However, the velocity of the corner layer in this phase of the phenomenon is determined by the type L asymptotics previously developed, i.e. by $\delta_L(p)$, which in turn depends on the initial condition.

6 Conclusions

The numerical investigation of viscous gravity currents starting from initial conditions of the type $h \propto x^p$ gives results in harmony with theory. The agreement with experiments on the spreading of viscous liquids (discounting surface tension and two-dimensional effects) is good. If $p < 2/m = 2/3$, start-up is immediate. If $p > 2/3$ there is a finite waiting-time. During the waiting stage the profile distorts until a moving corner layer develops; as the corner layer advances towards the front it strengthens. Power-law initial profiles yield waiting-time solutions with a single corner layer. Start-up occurs when the corner layer overtakes the front. The point source solution gives a reasonably good estimate (by excess) of the waiting-time, except for p close to $2/3$.

In addition to the exact numerical value of the waiting-time, the numerical solutions yield a wealth of new results concerning the properties of waiting-time solutions, especially regarding the self-similarity of the asymptotic behavior in certain domains. These features are impossible to observe in the experiments, since the measurements cannot be sufficiently precise, and perturbing effects are always present. The asymptotics of the solutions of (1), (3) near the front and to start-up is self-similar of the second kind, and consists of two domains. In the neighborhood of the front the asymptotics is of type A, with $\delta = 1$, the velocity of the front is discontinuous at start-up. In an intermediate domain a type L asymptotics with $\delta = \delta_L(p)$, $(1 < \delta_L(p) < 13/10)$ occurs. The initial condition determines δ_L. The type L solutions have an infinite number of corner layers, but since the solution of the initial value problem tends very slowly to its asymptotics where h is small, with the initial conditions (3) the first corner layer arrives too rapidly to the front (ending the waiting stage), not allowing the development of other corner layers. Furthermore, as the corner layer approaches the front and strengthens, the main flow becomes independent of the conditions downstream and tends to a constant velocity asymptotics (with c determined by the initial condition). The LOT solutions of types S and N are unstable and do not represent the asymptotics of any real problem. Some of the present results await theoretical explanations and suggest directions for further research.

Acknowledgement

We acknowledge many helpful discussions with Professors A. B. Tayler, J. R. Ockendon, J. King, L. A. Peletier, R. Gratton and F. Minotti. This work was supported by CONICET, by Grant EX245 of the University of Buenos Aires and by the EC Contract/Grant No. CTI*CT91-0944.

References

ARONSON, D. G. (1970) Regularity properties of flows through porous media: A counterexample. *SIAM J. Appl. Math.*, **19**, 299–307.

ARONSON, D. G. & VÁZQUEZ, J. L. (1994) Calculation of anomalous exponents in nonlinear diffusion. *Phys. Rev. Lett.*, **72**, 348–351.

ARONSON, D. G., CAFFARELLI, L. A. & KAMIN, S. (1983) How an initially stationary interface begins to move in porous medium flow 1983. *SIAM J. Math. Anal.*, **14**, 639–658.

ARONSON, D. G., CAFFARELLI, L. A. & VÁZQUEZ, J. L. (1985) Interfaces with a corner point in one-dimensional porous medium flow. *Comm. Pure Appl. Math.*, **38**, 375–404.

BARENBLATT, G. I. (1952) One some unsteady motions of fluids and gases in a porous medium. *Prikl. Mat. i Mekh.*, **16**(1), 67–78.

BARENBLATT, G. I. (1979) *Similarity, Self-Similarity and Intermediate Asymptotics.* Consultant Bureau, New York and London.

BARENBLATT, G. I. & ZEL'DOVICH, YA. B. (1957) On the dipole-type solution in problems of unsteady gas filtration in the polytropic regime. *Prikl. Mat. i Mekh.*, **21**, 718–720.

BARENBLATT, G. I. & ZEL'DOVICH, YA. B. (1972) Self-similar solutions as intermediate asymptotics. *Ann. Rev. Fluid Mech.*, **4**, 295–312.

BUCKMASTER, J. (1977) Viscous sheets advancing over dry beds. *J. Fluid Mech.*, **81**, 735–756.

DEL CARMEN, A. & FERRERI, J. C. (1995) Numerical solutions of viscous, waiting, gravity driven flows. *Física de Fluidos 95*, 113–127. CIC.

EAGLESON, P. S. (1970) *Dynamic Hydrology.* McGraw-Hill.

GILDING, B. H. & PELETIER, L. A. (1977a) On a class of similarity solutions of the porous media equations. *J. Math. Anal. Appl.*, **55**, 351–364.

GILDING, B. H. & PELETIER, L. A. (1977b) On a class of similarity solutions of the porous media equations II. *J. Math. Anal. Appl.*, **57**, 522–538.

GRATTON, J. & VIGO, C. (1994a) Asintótica autosemejante de flujos viscogravitatorios con tiempo de espera en función del perfil inicial. *Anales AFA*, **6**, 315–319.

GRATTON, J. & VIGO, C. (1994b) Soluciones autosemejantes con tiempo de espera de ecuaciones no lineales de difusión. *Anales AFA*, **6**, 326–331.

GRATTON, J. & MINOTTI, F. (1990) Self-similar viscous gravity currents: phase plane formalism. *J. Fluid Mech.*, **210**, 155–182.

GRATTON, J., ROSSELLO, E. & DIEZ, J. (1992) Physical modeling of free flows: waiting-time behavior. *Mon. Ac. Nac. Ciencias Exactas Fis. y Nat.*, **8**, 51–63.

GRUNDY, R. E. (1979) Similarity solutions of the nonlinear diffusion equation. *Quart. Appl. Math.*, **37**, 259–280.

HIRT, C. W. & HARLOW, F. (1967) A general corrective procedure for the numerical solution of initial-value problems. *J. Comp. Phys.*, **2**, 114–119.

HUPPERT, H. E. (1982) The propagation of two-dimensional viscous gravity currents over a rigid horizontal surface. *J. Fluid Mech.*, **121**, 43–58.

KALNAY DE RIVAS, E. (1972) On the use of nonuniform grids in finite-difference equations. *J. Comp. Phys.*, **10**, 201–203.

KAMIN, S. (1980) Continuous groups of transformations of differential equations; applications to free boundary problems. In E. Magenes (ed.), *Free Boundary Problems*, Tecnoprint, Roma.

KATH, W. L. & COHEN, D. S. (1982) Waiting-time behavior in a nonlinear diffusion equation. *Stud. Appl. Math.*, **67**, 79–105.

KNERR, B. F. (1977) The porous medium equation in one dimension. *Trans. Am. Math. Soc.*, **234**, 381–415.

LACEY, A. A. (1983) Initial motion of the free boundary for a non-linear diffusion equation. *IMA J. Appl. Math.*, **31**, 113–119.

LACEY, A. A., OCKENDON, J. R. & TAYLER, A. B. (1982) "Waiting-time" solutions of a nonlinear diffusion equation. *J. Appl. Math.*, **42**, 1252–1264.

LARSEN, E. W. & POMRANING, G. C. (1980) Asymptotic analysis of nonlinear Marshak waves. *SIAM J. Appl. Math.*, **39**, 201–212.

MARINO, B. M., THOMAS, L. P., GRATTON, R., DIEZ, J. A., BETELÚ, S. & GRATTON, J. (1995) Waiting time solutions of a non-linear diffusion equation: experimental study of a creeping flow near a waiting front. *Phys. Rev. E* (in press).

MARSHAK, R. E. (1958) Effect of radiation on shock wave behavior. *Phys. Fluids*, **1**, 24–29.

MUSKAT, M. (1937) *The Flow of Homogeneous Fluids through Porous Media.* McGraw-Hill.

PATTLE, R. E. (1959) Diffusion from an instantaneous point source with a concentration-dependent coefficient. *Quart. J. Mech. Appl. Math.*, **12**, 407–409.

PELETIER, L. A. (1981) *Applications of Nonlinear Analysis in the Physical Sciences, Chap. 11. The Porous Media Equation.* Pitman Adv. Pub. Prog., Boston, pp. 229–240.

PERT, G. J. (1977) A class of similar solutions of the non-linear diffusion equation. *J. Phys. A: Math. Gen.*, **10**(4), 583–593.

POLUBARINOVA-KOCHINA, P. Y. (1962) *Theory of Ground Water Movement.* Princeton University Press.

THOMAS, L. P., DIEZ, J. A., MARINO, B. M., GRATTON, R. & GRATTON, J. (1991) Corrientes viscogravitatorias con frentes que esperan. *Anales AFA*, **3**, 213–216.

TOMOEDA, K. & MIMURA, M. (1983) Numerical approximations to interface curves for a porous media equation. *Hiroshima Math. J.*, **13**, 273–294.

VÁZQUEZ, J. L. (1983) Large time behavior of the solutions of the one-dimensional porous media equation. *Free Boundary Problems: Theory and Applications, Vol. I.* Pitman, Boston, pp. 167–177.

VÁZQUEZ, J. L. (1984) The interface of one-dimensional flows in porous media. *Trans. Amer. Math. Soc.*, **285**, 717–737.

ZEL'DOVICH, YA. B. & RAIZER, YU. P. (1966) *Physics of Shock Waves and High Temperature Hydrodynamic Phenomena.* Academic Press, New York.